Excerpt from Chapter 13 of:

Legendre, P. and L. Legendre. 1998. Numerical ecology, 2nd English edition. Elsevier Science BV, Amsterdam. xv + 853 pages.

13.1 Structure functions

Ecologists are interested in describing spatial structures in quantitative ways and testing for the presence of spatial autocorrelation in data. The primary objective is to:

- either support the null hypothesis that no significant spatial autocorrelation is present in a data set, or that none remains after detrending (Subsection 13.2.1) or after

Table 13.1 Surface pattern analysis: research objectives and related numerical methods. Modified from Legendre & Fortin (1989).

Research objective	Numerical methods
1) Description of spatial structures and testing for the presence of spatial autocorrelation (Descriptions using structure functions should always be complemented by maps.)	Univariate structure functions: correlogram, variogram, etc. (Section 13.1)
	Multivariate structure functions: Mantel correlogram (Section 13.1)
	Testing for a gradient in multivariate data: (1) constrained (canonical) ordination between the multivariate data and the geographic coordinates of the sites (Section 13.4). (2) Mantel test between ecological distances (computed from the multivariate data) and geographic distances (Subsection 10.5.1)
2) Mapping; estimation of values at given locations	Univariate data: local interpolation map; trend-surface map (global statistical model) (Sect. 13.2)
	Multivariate data: clustering with spatial contiguity constraint, search for boundaries (Section 13.3); interpolated map of the 1st (2nd, etc.) ordination axis (Section 13.4); multivariate trend-surface map obtained by constrained ordination (canonical analysis) (Section 13.4)
3) Modelling species-environment relationships while taking spatial structures into account	Raw data tables: partial canonical analysis (Section 13.5)
	Distance matrices: partial Mantel analysis (Section 13.6)
4) Performing valid statistical tests on autocorrelated data	Subsection 1.1.1

controlling for the effect of explanatory (e.g., environmental) variables, thus insuring valid use of the standard univariate or multivariate statistical tests of hypotheses.

• or reject the null hypothesis and show that significant spatial autocorrelation is present in the data, in order to use it in conceptual or statistical models.

Tests of spatial autocorrelation coefficients may only support or reject the null hypothesis of the absence of significant spatial structure. When significant spatial structure is found, it may correspond, or not, to spatial autocorrelation (Section 1.1, model b) — depending on the hypothesis of the investigator.

Map

Spatial structures may be described through *structure functions*, which allow one to quantify the spatial dependence and partition it amongst distance classes. Interpretation of this description is usually supported by maps of the univariate or multivariate data (Sections 13.2 to 13.4). The most commonly used structure functions are correlograms, variograms, and periodograms.

Spatial correlogram

A *correlogram* is a graph in which autocorrelation values are plotted, on the ordinate, against *distance classes* among sites on the abscissa. Correlograms (Cliff & Ord 1981) can be computed for single variables (Moran's I or Geary's c autocorrelation coefficients, Subsection 1) or for multivariate data (Mantel correlogram, Subsection 5); both types are described below. In all cases, a test of significance is available for each individual autocorrelation coefficient plotted in a correlogram.

Variogram

Similarly, a *variogram* is a graph in which semi-variance is plotted, on the ordinate, against *distance classes* among sites on the abscissa (Subsection 3). In the geostatistical tradition, semi-variance statistics are not tested for significance, although they could be through the test developed for Geary's c, when the condition of second-order stationarity is satisfied (Subsection 13.1.1). Statistical models may be fitted to variograms (linear, exponential, spherical, Gaussian, etc.); they allow the investigator to relate the observed structure to hypothesized generating processes or to produce interpolated maps by kriging (Subsection 13.2.2).

Because they measure the relationship between pairs of observation points located a certain distance apart, correlograms and variograms may be computed either for preferred geographic directions or, when the phenomenon is assumed to be isotropic in space, in an all-directional way.

2-D periodogram

A *two-dimensional Schuster* (1898) *periodogram* may be computed when the structure under study is assumed to consist of a combination of sine waves propagated through space. The basic idea is to fit sines and cosines of various periods, one period at a time, and to determine the proportion of the series' variance (r^2) explained by each period. In periodograms, the abscissa is either a period or its inverse, a frequency; the ordinate is the proportion of variance explained. Two-dimensional periodograms may be plotted for all combinations of directions and spatial frequencies. The technique is described Priestley (1964), Ripley (1981), Renshaw and Ford (1984) and Legendre & Fortin (1989). It is not discussed further in the present book.

1 — Spatial correlograms

For quantitative variables, spatial autocorrelation may be measured by either Moran's I (1950) or Geary's c (1954) spatial autocorrelation statistics (Cliff & Ord, 1981):

Moran's *I*:
$$I(d) = \frac{\frac{1}{W}\sum_{h=1}^{n}\sum_{i=1}^{n} w_{hi}(y_h - \bar{y})(y_i - \bar{y})}{\frac{1}{n}\sum_{i=1}^{n}(y_i - \bar{y})^2} \quad \text{for } h \neq i \qquad \textbf{(13.1)}$$

Geary's *c*:
$$c(d) = \frac{\frac{1}{2W}\sum_{h=1}^{n}\sum_{i=1}^{n} w_{hi}(y_h - y_i)^2}{\frac{1}{(n-1)}\sum_{i=1}^{n}(y_i - \bar{y})^2} \quad \text{for } h \neq i \qquad \textbf{(13.2)}$$

The y_h's and y_i's are the values of the observed variable at sites h and i. Before computing spatial autocorrelation coefficients, a matrix of geographic distances $\mathbf{D} = [D_{hi}]$ among observation sites must be calculated. In the construction of a correlogram, spatial autocorrelation coefficients are computed, in turn, for the various distance classes d. The weights w_{hi} are Kronecker deltas (as in eq. 7.20); the weights take the value $w_{hi} = 1$ when sites h and i are at distance d and $w_{hi} = 0$ otherwise. In this way, only the pairs of sites (h, i) within the stated distance class (d) are taken into account in the calculation of any given coefficient. This approach is illustrated in Fig. 13.3. W is the sum of the weights w_{hi} for the given distance class, i.e. the number of pairs used to calculate the coefficient. For a given distance class, the weights w_{ij} are written in a $(n \times n)$ matrix **W**. Jumars *et al.* (1977) present ecological examples where the distance^{-1} or distance^{-2} among adjacent sites is used for weight instead of 1's.

The numerators of eqs. 13.1 and 13.2 are written with summations involving each pair of objects twice; in eq. 13.2 for example, the terms $(y_h - y_i)^2$ and $(y_i - y_h)^2$ are both used in the summation. This allows for cases where the distance matrix **D** or the weight matrix **W** is asymmetric. In studies of the dispersion of pollutants in soil, for instance, drainage may make it more difficult to go from A to B than from B to A; this may be recorded as a larger distance from A to B than from B to A. In spatio-temporal analyses, an observed value may influence a later value at the same or a different site, but not the reverse. An impossible connection may be coded by a very large value of distance. In most applications, however, the geographic distance matrix among sites is symmetric and the coefficients may be computed from the half-matrix of distances; the formulae remain the same, in that case, because W, as well as the sum in the numerator, are half the values computed over the whole distance matrix **D** (except $h = i$).

One may use distances along a network of connections (Subsection 13.3.1) instead of straight-line geographic distances; this includes the "chess moves" for regularly-spaced points as obtained from systematic sampling designs: rook's, bishop's, or king's connections (see Fig. 13.19). For very broad-scale studies, involving a whole ocean for instance, "great-circle distances", i.e. distances along earth's curved surface, should be used instead of straight-line distances through the earth crust.

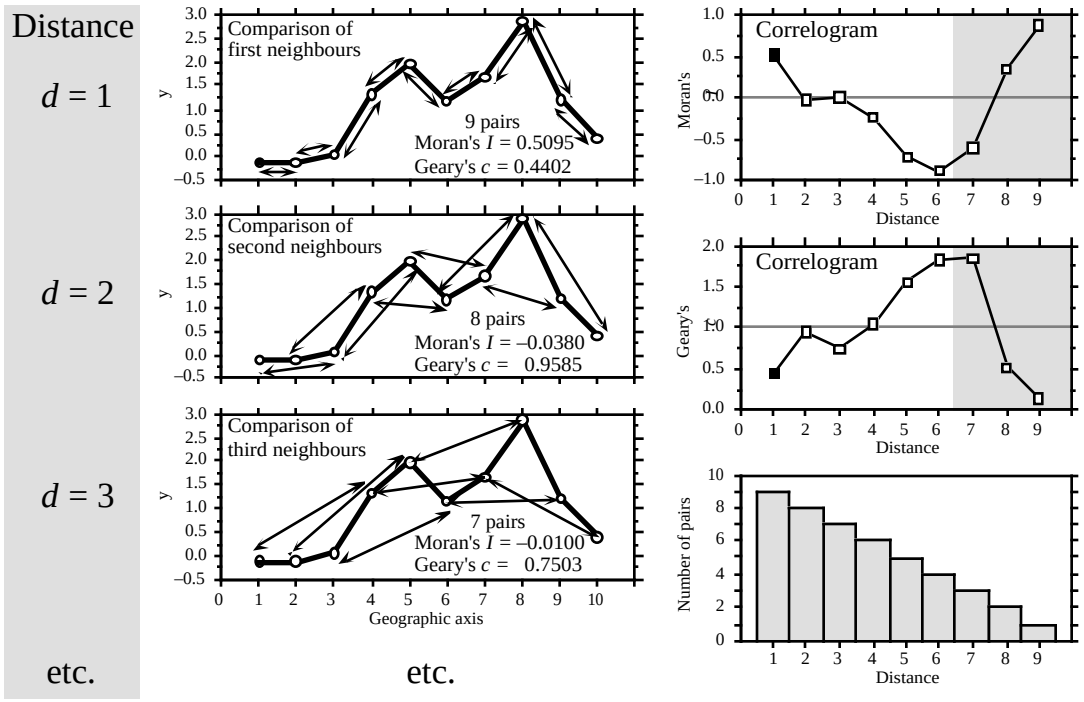

Figure 13.3 Construction of correlograms. Left: data series observed along a single geographic axis (10 equispaced observations). Moran's I and Geary's c statistics are computed from pairs of observations found at preselected distances ($d = 1$, $d = 2$, $d = 3$, etc.). Right: correlograms are graphs of the autocorrelation statistics plotted against distance. Dark squares: significant autocorrelation statistics ($p \leq 0.05$). Lower right: histogram showing the number of pairs in each distance class. Coefficients for the larger distance values (grey zones in correlograms) should not be considered in correlograms, nor interpreted, because they are based on a small number of pairs (test with low power) and only include the pairs of points bordering the series or surface.

Moran's I formula is related to Pearson's correlation coefficient; its numerator is a covariance, comparing the values found at all pairs of points in turn, while its denominator is the maximum-likelihood estimator of the variance (i.e. division by n instead of $n - 1$); in Pearson's r, the denominator is the product of the standard deviations of the two variables (eq. 4.7), whereas in Moran's I there is only one variable involved. Moran's I mainly differs from Pearson's r in that the sums in the numerator and denominator of eq. 13.1 do not involve the same number of terms; only the terms corresponding to distances within the given class are considered in the numerator whereas all pairs are taken into account in the denominator. Moran's I usually takes values in the interval [–1, +1] although values lower than –1 or higher than +1 may occasionally be obtained. Positive autocorrelation in the data translates into positive values of I; negative autocorrelation produces negative values.

Readers who are familiar with correlograms in time series analysis will be reassured to know that, when a problem involves equispaced observations along a single physical dimension, as in Fig. 13.3, calculating Moran's I for the different distance classes is nearly the same as computing the autocorrelation coefficient of time series analysis (Fig. 12.5, eq. 12.6); a small numeric difference results from the divisions by $(n-k-1)$ and $(n-1)$, respectively, in the numerator and denominator of eq. 12.6, whereas division is by $(n-k)$ and (n), respectively, in the numerator and denominator of Moran's I formula (eq. 13.1).

Geary's c coefficient is a distance-type function; it varies from 0 to some unspecified value larger than 1. Its numerator sums the squared differences between values found at the various pairs of sites being compared. A Geary's c correlogram varies as the reverse of a Moran's I correlogram; strong autocorrelation produces high values of I and low values of c (Fig. 13.3). Positive autocorrelation translates in values of c between 0 and 1 whereas negative autocorrelation produces values larger than 1. Hence, the reference 'no correlation' value is $c = 1$ in Geary's correlograms.

For sites lying on a surface or in a volume, geographic distances do not naturally fall into a small number of values; this is true for regular grids as well as random or other forms of irregular sampling designs. Distance values must be grouped into distance classes; in this way, each spatial autocorrelation coefficient can be computed using several comparisons of sampling sites.

Numerical example. In Fig. 13.4 (artificial data), 10 sites have been located at random into a 1-km^2 sampling area. Euclidean (geographic) distances were computed among sites. The number of classes is arbitrary and left to the user's decision. A compromise has to be made between resolution of the correlogram (more resolution when there are more, narrower classes) and power of the test (more power when there are more pairs in a distance class). Sturge's rule is often used to decide about the number of classes in histograms; it was used here and gave:

$$\text{Number of classes} = 1 + 3.322 \log_{10}(m) = 1 + 3.3 \log_{10}(45) = 6.46 \qquad \textbf{(13.3)}$$

where m is the number of distances in the upper triangular matrix and 3.322 is $1/\log_{10}2$; the number was rounded to the nearest integer (i.e. 6). The distance matrix was thus recoded into 6 classes, ascribing class numbers (1 to 6) to all distances within a class of the histogram.

An alternative to distance classes with equal widths would be to create distance classes containing the same number of pairs (notwithstanding tied values); distance classes formed in this way are of unequal widths. The advantage is that the tests of significance have the same power across all distance classes because they are based upon the same number of pairs of observations. The disadvantages are that limits of the distance classes are more difficult to find and correlograms are harder to draw.

Spatial autocorrelation coefficients can be tested for significance and confidence intervals can be computed. With proper correction for multiple testing, one can determine whether a significant spatial structure is present in the data and what are the distance classes showing significant positive or negative autocorrelation. Tests of significance require, however, that certain conditions specified below be fulfilled.

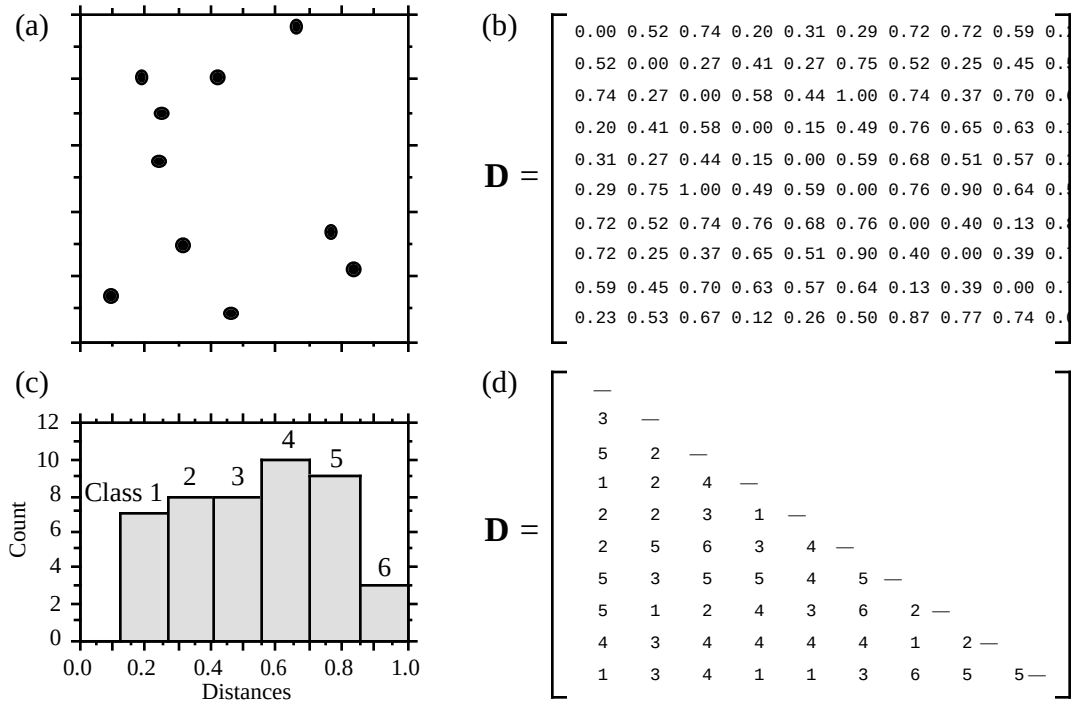

Figure 13.4 Calculation of distance classes, artificial data. (a) Map of 10 sites in a 1-km^2 sampling area. (b) Geographic distance matrix (**D**, in km). (c) Frequency histogram of distances (classes 1 to 6) for the upper (or lower) triangular portion of **D**. (d) Distances recoded into 6 classes.

Second-order stationarity

The tests require that the condition of *second-order stationarity* be satisfied. This rather strong condition states that the expected value (mean) and spatial covariance (numerator of eq. 13.1) of the variable is the same all over the study area, and the variance (denominator of eq. 13.1) is finite. The value of the autocorrelation function depends only on the length and orientation of the vector between any two points, not on its position in the study area (David, 1977).

Intrinsic assumption

A relaxed form of stationarity hypothesis, the *intrinsic assumption*, states that the differences $(y_h - y_i)$ for any distance d (in the numerator of eq. 13.2) must have zero mean and constant and finite variance over the study area, independently of the location where the differences are calculated. Here, one considers the *increments* of the values of the regionalized variable instead of the values themselves (David, 1977). As shown below, the variance of the increments is the variogram function. In layman's terms, this means that a single autocorrelation function is adequate to describe the entire surface under study. An example where the intrinsic assumption does not hold is

a region which is half plain and half mountains; such a region should be divided in two subregions in which the variable "altitude" could be modelled by separate autocorrelation functions. This condition must always be met when variograms or correlograms (including multivariate Mantel correlograms) are computed, even for descriptive purpose.

Cliff & Ord (1981) describe how to compute confidence intervals and test the significance of spatial autocorrelation coefficients. For any normally distributed statistic *Stat*, a confidence interval at significance level α is obtained as follows:

$$Pr\,(Stat - z_{\alpha/2}\sqrt{\mathrm{Var}\,(Stat)} < Stat_{\mathrm{Pop}} < Stat + z_{\alpha/2}\sqrt{\mathrm{Var}\,(Stat)}) \;=\; 1-\alpha \qquad \textbf{(13.4)}$$

For significance testing with large samples, a one-tailed critical value $Stat_\alpha$ at significance level α is obtained as follows:

$$Stat_\alpha = z_\alpha\sqrt{\mathrm{Var}\,(Stat)} + \text{Expected value of } Stat \text{ under } \mathrm{H}_0 \qquad \textbf{(13.5)}$$

It is possible to use this approach because both I and c are asymptotically normally distributed for data sets of moderate to large sizes (Cliff & Ord, 1981). Values $z_{\alpha/2}$ or z_α are found in a table of standard normal deviates. Under the hypothesis (H_0) of random spatial distribution of the observed values y_i, the expected values (E) of Moran's I and Geary's c are:

$$\mathrm{E}(I) = -(n-1)^{-1} \quad \text{and} \quad \mathrm{E}(c) = 1 \qquad \textbf{(13.6)}$$

Under the null hypothesis, the expected value of Moran's I approaches 0 as n increases. The variances are computed as follows under a randomization assumption, which simply states that, under H_0, the observations y_i are independent of their positions in space and, thus, are exchangeable:

$$\mathrm{Var}\,(I) \;=\; \mathrm{E}(I^2) - [\mathrm{E}(I)]^2 \qquad \textbf{(13.7)}$$

$$\mathrm{Var}\,(I) \;=\; \frac{n\,[(n^2-3n+3)\,S_1 - nS_2 + 3W^2] - b_2\,[(n^2-n)\,S_1 - 2nS_2 + 6W^2]}{(n-1)\,(n-2)\,(n-3)\,W^2} - \frac{1}{(n-1)^2}$$

$$\mathrm{Var}\,(c) \;=\; \frac{(n-1)\,S_1\,[n^2-3n+3-(n-1)\,b_2]}{n\,(n-2)\,(n-3)\,W^2} \qquad \textbf{(13.8)}$$

$$+\;\frac{-0.25\,(n-1)\,S_2\,[n^2+3n-6-(n^2-n+2)\,b_2] + W^2\,[n^2-3+(-(n-1)^2)\,b_2]}{n\,(n-2)\,(n-3)\,W^2}$$

In these equations,

- $S_1 = \frac{1}{2}\sum_{h=1}^{n}\sum_{i=1}^{n}(w_{hi} + w_{ih})^2$ (there is a term of this sum for *each cell* of matrix **W**);
- $S_2 = \sum_{i=1}^{n}(w_{i+} + w_{+i})^2$ where w_{i+} and w_{+i} are respectively the sums of row i and column i of matrix **W**;
- $b_2 = n\sum_{i=1}^{n}(y_i - \bar{y})^4 / \left[\sum_{i=1}^{n}(y_i - \bar{y})^2\right]^2$ measures the kurtosis of the distribution;
- W is as defined in eqs. 13.1 and 13.2.

In most cases in ecology, tests of spatial autocorrelation are one-tailed because the sign of autocorrelation is stated in the ecological hypothesis; for instance, contagious biological processes such as growth, reproduction, and dispersal, all suggest that ecological variables are positively autocorrelated at short distances. To carry out an approximate test of significance, select a value of α (e.g. $\alpha = 0.05$) and find z_α in a table of the standard normal distribution (e.g. $z_{0.05} = +1.6452$). Critical values are found as in eq. 13.5, with a correction factor that becomes important when n is small:

- $I_\alpha = z_\alpha\sqrt{\mathrm{Var}(I)} - k_\alpha(n-1)^{-1}$ in all cases, using the value in the upper tail of the z distribution when testing for positive autocorrelation (e.g. $z_{0.05} = +1.6452$) and the value in the lower tail in the opposite case (e.g. $z_{0.05} = -1.6452$).

- $c_\alpha = z_\alpha\sqrt{\mathrm{Var}(c)} + 1$ when $c < 1$ (positive autocorrelation), using the value in the lower tail of the z distribution (e.g. $z_{0.05} = -1.6452$).

- $c_\alpha = z_\alpha\sqrt{\mathrm{Var}(c)} + 1 - k_\alpha(n-1)^{-1}$ when $c > 1$ (negative autocorrelation), using the value in the upper tail of the z distribution (e.g. $z_{0.05} = +1.6452$).

The value taken by the correction factor k_α depends on the values of n and W. If $4(n - \sqrt{n}) < W \leq 4(2n - 3\sqrt{n} + 1)$, then $k_\alpha = \sqrt{10\alpha}$; otherwise, $k_\alpha = 1$. If the test is two-tailed, use $\alpha^* = \alpha/2$ to find z_{α^*} and k_{α^*} before computing critical values. These corrections are based upon simulations reported by Cliff & Ord (1981, section 2.5).

Other formulas are found in Cliff & Ord (1981) for conducting a test under the assumption of normality, where one assumes that the y_i's result from n independent draws from a normal population. When n is very small, tests of I and c should be conducted by randomization (Section 1.2).

Moran's I and Geary's c are sensitive to extreme values and, in general, to asymmetry in the data distributions, as are the related Pearson's r and Euclidean distance coefficients. Asymmetry increases the variance of the data. It also increases the kurtosis and hence the variance of the I and c coefficients (eqs. 13.7 and 13.8); this

makes it more difficult to reach significance in statistical tests. So, practitioners usually attempt to normalize the data before computing correlograms and variograms.

Statistical testing in correlograms implies multiple testing since a test of significance is carried out for each autocorrelation coefficient. Oden (1984) has developed a Q statistic to test the global significance of spatial correlograms; his test is an extension of the Portmanteau Q-test used in time series analysis (Box & Jenkins, 1976). An alternative global test is to check whether the correlogram contains at least one autocorrelation statistic which is significant at the Bonferroni-corrected significance level (Box 1.3). Simulations in Oden (1984) show that the power of the Q-test is not appreciably greater than the power of the Bonferroni procedure, which is computationally a lot simpler. A practical question remains, though: how many distance classes should be created? This determines the number of simultaneous tests that are carried out. More classes mean more resolution but fewer pairs per class and, thus, less power for each test; more classes also mean a smaller Bonferroni-corrected α' level, which makes it more difficult for a correlogram to reach global significance.

When the overall test has shown global significance, one may wish to identify the individual autocorrelation statistics that are significant, in order to reach an interpretation (Subsection 2). One could rely on Bonferroni-corrected tests for all individual autocorrelation statistics, but this approach would be too conservative; a better solution is to use Holm's correction procedure (Box 1.3). Another approach is the *progressive Bonferroni correction* described in Subsection 12.4.2; it is only applicable when the ecological hypothesis indicates that significant autocorrelation is to be expected in the smallest distance classes and the purpose of the analysis is to determine the extent of the autocorrelation (i.e. which distance class it reaches). With the progressive Bonferroni approach, the likelihood of emergence of significant values decreases as one proceeds from left to right, i.e. from the small to the large distance classes of the correlogram. One does not have to limit the correlogram to a small number of classes to reduce the effect of the correction, as it is the case with Oden's overall test and with the Bonferroni and Holm correction methods. This approach will be used in the examples that follow.

Autocorrelation coefficients and tests of significance also exist for qualitative (nominal) variables (Cliff & Ord 1981); they have been used to analyse for instance spatial patterns of sexes in plants (Sakai & Oden 1983; Sokal & Thomson 1987). Special types of spatial autocorrelation coefficients have been developed to answer specific problems (e.g. Galiano 1983; Estabrook & Gates 1984). The paired-quadrat variance method, developed by Goodall (1974) to analyse spatial patterns of ecological data by random pairing of quadrats, is related to correlograms.

2 — Interpretation of all-directional correlograms

Isotropy
Anisotropy

When the autocorrelation function is the same for all geographic directions considered, the phenomenon is said to be *isotropic*. Its opposite is *anisotropy*. When a variable is isotropic, a single correlogram may be computed over all directions of the

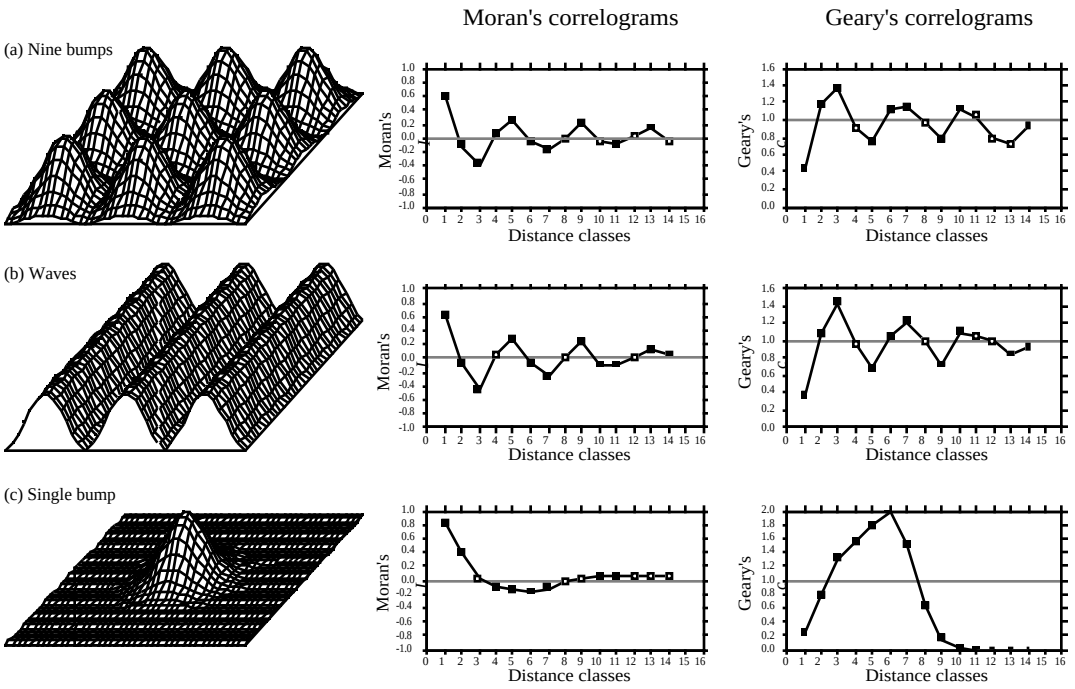

Figure 13.5 Spatial autocorrelation analysis of artificial spatial structures shown on the left: (a) nine bumps; (b) waves; (c) a single bump. Centre and right: all-directional correlograms. Dark squares: autocorrelation statistics that remain significant after progressive Bonferroni correction ($\alpha = 0.05$); white squares: non-significant values.

study area. The correlogram is said to be *all-directional* or *omnidirectional*. Directional correlograms, which are computed for a single direction of space, are discussed together with anisotropy and directional variograms in Subsection 3.

Correlograms are analysed mostly by looking at their shapes. Examples will help clarify the relationship between spatial structures and all-directional correlograms. The important message is that, although correlograms may give clues as to the underlying spatial structure, the information they provide is not specific; a blind interpretation may often be misleading and should always be supported by maps (Section 13.2).

Numerical example. Artificial data were generated that correspond to a number of spatial patterns. The data and resulting correlograms are presented in Fig. 13.5.

• Nine bumps — The surface in Fig. 13.5a is made of nine bi-normal curves. 225 points were sampled across the surface using a regular 15×15 grid (Fig. 13.5f). The "height" was noted at each sampling point. The 25 200 distances among points found in the upper-triangular portion of the distance matrix were divided into 16 distance classes, using Sturge's rule (eq. 13.3), and

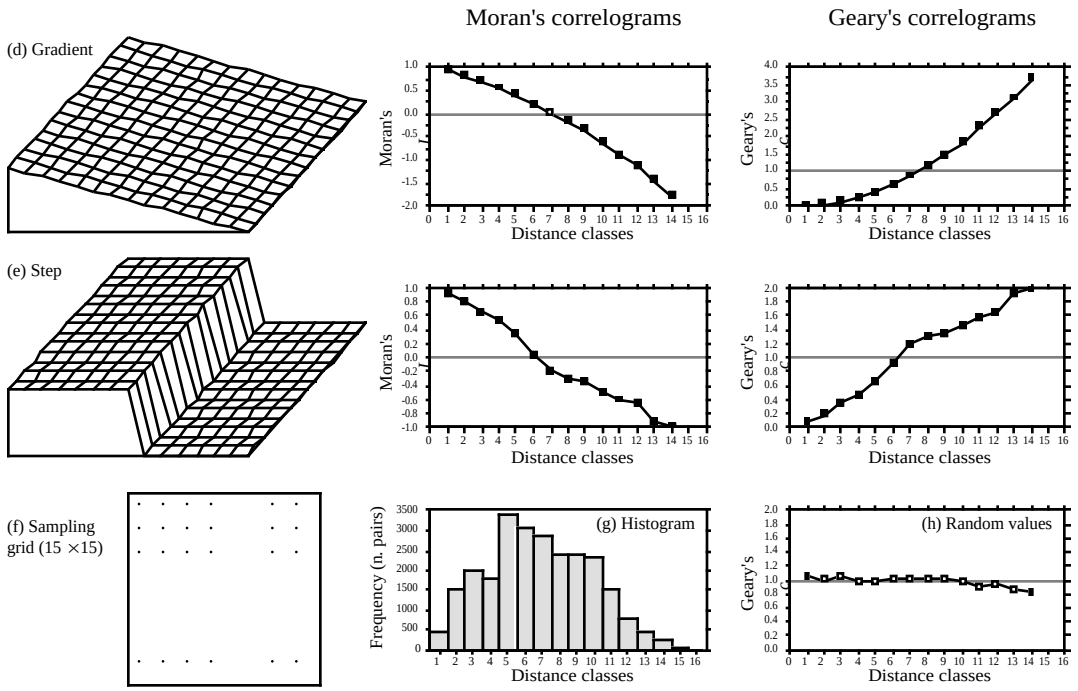

Figure 13.5 **(continued)** Spatial autocorrelation analysis of artificial spatial structures shown on the left: (d) gradient; (e) step. (h) All-directional correlogram of random values. (f) Sampling grid used on each of the artificial spatial structures to obtain 225 "observed values" for spatial autocorrelation analysis. (g) Histogram showing the number of pairs in each distance class. Distances, from 1 to 19.8 in units of the sampling grid, were grouped into 16 distance classes. Spatial autocorrelation statistics (I or c) are not shown for distance classes 15 and 16; see text.

correlograms were computed. According to Oden's test, the correlograms are globally significant at the $\alpha = 5\%$ level since several individual values are significant at the Bonferroni-corrected level $\alpha' = 0.05/16 = 0.00312$. In each correlogram, the progressive Bonferroni correction method was applied to identify significant spatial autocorrelation coefficients: the coefficient for distance class 1 was tested at the $\alpha = 0.05$ level; the coefficient for distance class 2 was tested at the $\alpha' = 0.05/2$ level; and, more generally, the coefficient for distance class k was tested at the $\alpha' = 0.05/k$ level. Spatial autocorrelation coefficients are not reported for distance classes 15 and 16 (60 and 10 pairs, respectively) because they only include the pairs of points bordering the surface, to the exclusion of all other pairs.

There is a correspondence between individual significant spatial autocorrelation coefficients and the main elements of the spatial structure. The correspondence can clearly be seen in this example, where the data generating process is known. This is not the case when analysing field data, in which case the existence and nature of the spatial structures must be confirmed by mapping the data. The presence of several equispaced patches produces an alternation of

significant positive and negative values along the correlograms. The first spatial autocorrelation coefficient, which is above 0 in Moran's correlogram and below 1 in Geary's, indicates positive spatial autocorrelation in the first distance class; the first class contains the 420 pairs of points that are at distance 1 of each other on the grid (i.e. the first neighbours in the N-S or E-W directions of the map). Positive and significant spatial autocorrelation in the first distance class confirms that the distance between first neighbours is smaller than the patch size; if the distance between first neighbours in this example was larger than the patch size, first neighbours would be dissimilar in values and autocorrelation would be negative for the first distance class. The next peaking positive autocorrelation value (which is smaller than 1 in Geary's correlogram) occurs at distance class 5, which includes distances from 4.95 to 6.19 in grid units; this corresponds to positive autocorrelation between points located at similar positions on neighbouring bumps, or neighbouring troughs; distances between successive peaks are 5 grid units in the E-W or N-S directions. The next peaking positive autocorrelation value occurs at distance class 9 (distances from 9.90 to 11.14 in grid units); it includes value 10, which is the distance between second-neighbour bumps in the N-S and E-W directions. Peaking negative autocorrelation values (which are larger than 1 in Geary's correlogram) are interpreted in a similar way. The first such value occurs at distance class 3 (distances from 2.48 to 3.71 in grid units); it includes value 2.5, which is the distance between peaks and troughs in the N-S and E-W directions on the map. If the bumps were unevenly spaced, the correlograms would be similar for the small distance classes, but there would be no other significant values afterwards.

The main problem with all-directional correlograms is that the diagonal comparisons are included in the same calculations as the N-S and E-W comparisons. As distances become larger, diagonal comparisons between, say, points located near the top of the nine bumps tend to fall in different distance classes than comparable N-S or E-W comparisons. This blurs the signal and makes the spatial autocorrelation coefficients for larger distance classes less significant and interpretable.

• Wave (Fig. 13.5b) — Each crest was generated as a normal curve. Crests were separated by five grid units; the surface was constructed in this way to make it comparable to Fig. 13.5a. The correlograms are nearly indistinguishable from those of the nine bumps. All-directional correlograms alone cannot tell apart regular bumps from regular waves; directional correlograms or maps are required.

• Single bump (Fig. 13.5c) — One of the normal curves of Fig. 13.5a was plotted alone at the centre of the study area. Significant negative autocorrelation, which reaches distance classes 6 or 7, delimits the extent of the "range of influence" of this single bump, which covers half the study area. It is not limited here by the rise of adjacent bumps, as this was the case in (a).

• Linear gradient (Fig. 13.5d) — The correlogram is monotonic decreasing. Nearly all autocorrelation values in the correlograms are significant.

True, false gradient

There are actually two kinds of gradients (Legendre, 1993). "True gradients", on the one hand, are deterministic structures. They correspond to generating model 2 of Subsection 1.1.1 (eq. 1.2) and can be modelled using trend-surface analysis (Subsection 13.2.1). The observed values have independent error terms, i.e. error terms which are not autocorrelated. "False gradients", on the other hand, are structures that may look like gradients, but actually correspond to autocorrelation generated by some spatial process (model 1 of Subsection 1.1.1; eq. 1.1). When the sampling area is small relative to the range of influence of the generating process, the data generated by such a process may look like a gradient.

In the case of "true gradients", spatial autocorrelation coefficients should not be tested for significance because the condition of second-order stationarity is not satisfied (definition in previous Subsection); the expected value of the mean is not the same over the whole study area. In the case of "false gradients", however, tests of significance are warranted. For descriptive purposes, correlograms may still be computed for "true gradients" (without tests of significance) because the intrinsic assumption is satisfied. One may also choose to extract a "true gradient" using trend-surface analysis, compute residuals, and look for spatial autocorrelation among the residuals. This is equivalent to trend extraction prior to time series analysis (Section 12.2).

How does one know whether a gradient is "true" or "false"? This is a moot point. When the process generating the observed structure is known, one may decide whether it is likely to have generated spatial autocorrelation in the observed data, or not. Otherwise, one may empirically look at the *target population* of the study. In the case of a spatial study, this is the population of potential sites in the larger area into which the study area is embedded, the study area representing the *statistical population* about which inference can be made. Even from sparse or indirect data, a researcher may form an opinion as to whether the observed gradient is deterministic ("true gradient") or is part of a landscape displaying autocorrelation at broader spatial scale ("false gradient").

• Step (Fig. 13.5e) — A step between two flat surfaces is enough to produce a correlogram which is indistinguishable, for all practical purposes, from that of a gradient. Correlograms alone cannot tell apart regular gradients from steps; maps are required. As in the case of gradients, there are "true steps" (deterministic) and "false steps" (resulting from an autocorrelated process), although the latter is rare. The presence of a sharp discontinuity in a surface generally indicates that the two parts should be subjected to separate analyses. The methods of boundary detection and constrained clustering (Section 13.3) may help detect such discontinuities and delimit homogeneous areas prior to spatial autocorrelation analysis.

• Random values (Fig. 13.5h) — Random numbers, drawn from a standard normal distribution, were generated for each point of the grid and used as the variable to be analysed. Random data are said to represent a "pure nugget effect" in geostatistics. The autocorrelation coefficients were small and non-significant at the 5% level. Only the Geary correlogram is presented.

Sokal (1979) and Cliff & Ord (1981) describe, in general terms, where to expect significant values in correlograms, for some spatial structures such as gradients and large or small patches. Their summary tables are in agreement with the test examples above. The absence of significant coefficients in a correlogram must be interpreted with caution, however:

• It may indicate that the surface under study is free of spatial autocorrelation at the study scale. Beware: this conclusion is subject to type II (or β) error. Type II error depends on the power of the test which is a function of (1) the α significance level, (2) the size of effect (i.e. the minimum amount of autocorrelation) one wants to detect, (3) the number of observations (n), and (4) the variance of the sample (Cohen, 1988):

$$\text{Power} = (1 - \beta) = f(\alpha, \text{size of effect}, n, s_x)$$

Is the test powerful enough to warrant such a conclusion? Are there enough observations to reach significance? The easiest way to increase the power of a test, for a given variable and fixed α, is to increase n.

• It may indicate that the sampling design is inadequate to detect the spatial autocorrelation that may exist in the system. Are the grain size, extent and sampling interval (Section 13.0) adequate to detect the type of autocorrelation one can hypothesize from knowledge about the biological or ecological process under study?

Ecologists can often formulate hypotheses about the mechanism or process that may have generated a spatial phenomenon and deduct the shape that the resulting surface should have. When the model specifies a value for each geographic position (e.g. a spatial gradient), data and model can be compared by correlation analysis. In other instances, the biological or ecological model only specifies process generating the spatial autocorrelation, not the exact geographic position of each resulting value. Correlograms may be used to support or reject the biological or ecological hypothesis. As in the examples of Fig. 13.5, one can construct an artificial model-surface corresponding to the hypothesis, compute a correlogram of that surface, and compare the correlograms of the real and model data. For instance, Sokal *et al.* (1997a) generated data corresponding to several gene dispersion mechanisms in populations and showed the kind of spatial correlogram that may be expected from each model. Another application concerning phylogenetic patterns of human evolution in Eurasia and Africa (space-time model) is found in Sokal *et al.* (1997b).

Bjørnstad & Falck (1997) and Bjørnstad *et al.* (1998) proposed a spline correlogram which provides a continuous and model-free function for the spatial covariance. The spline correlogram may be seen as a modification of the nonparametric covariance function of Hall and co-workers (Hall & Patil, 1994; Hall *et al.*, 1994). A bootstrap algorithm estimates the confidence envelope of the entire correlogram or derived statistics. This method allows the statistical testing of the similarity between correlograms of real and simulated (i.e. model) data.

Ecological application 13.1a

During a study of the factors potentially responsible for the choice of settling sites of *Balanus crenatus* larvae (Cirripedia) in the St. Lawrence Estuary (Hudon *et al.*, 1983), plates of artificial substrate (plastic laminate) were subjected to colonization in the infralittoral zone. Plates were positioned vertically, parallel to one another. A picture was taken of one of the plates after a 3-month immersion at a depth of 5 m below low tide, during the summer 1978. The picture was divided into a (10×15) grid, for a total of 150 pixels of 1.7×1.7 cm. Barnacles were counted by C. Hudon and P. Legendre for the present Ecological application (Fig. 13.6a; unpublished *in op. cit.*). The hypothesis to be tested is that barnacles have a patchy distribution. Barnacles are gregarious animals; their larvae are chemically attracted to settling sites by arthropodine secreted by settled adults (Gabbott & Larman, 1971).

A gradient in larval concentration was expected in the top-to-bottom direction of the plate because of the known negative phototropism of barnacle larvae at the time of settlement (Visscher, 1928). Some kind of border effect was also expected because access to the centre of the plates located in the middle of the pack was more limited than to the fringe. These large-scale effects create violations to the condition of second-order stationarity. A trend-surface equation (Subsection 13.2.1) was computed to account for it, using only the Y coordinate (top-

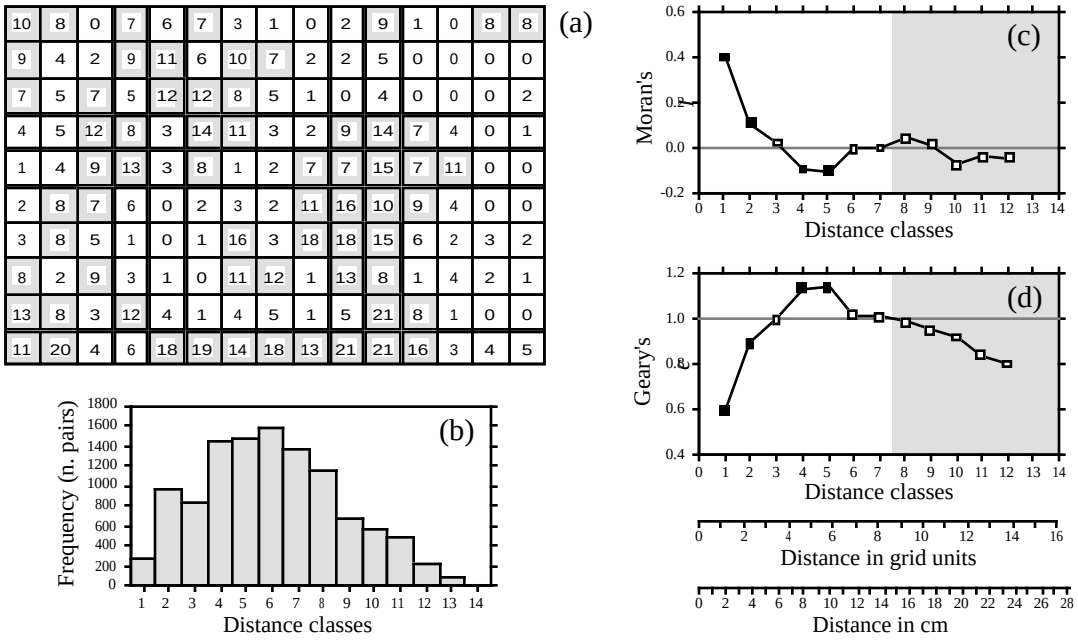

Figure 13.6 (a) Counts of adult barnacles in 150 (1.7×1.7 cm) pixels on a plate of artificial substrate (17×25.5 cm). The mean concentration is 6.17 animals per pixel; pixels with counts ≥ 7 are shaded to display the aggregates. (b) Histogram of the number of pairs in each distance class. (c) Moran's correlogram. (d) Geary's correlogram. Dark squares: autocorrelation statistics that remain significant after progressive Bonferroni correction ($\alpha = 0.05$); white squares: non-significant values. Coefficients for distance classes 13 and 14 are not given because they only include the pairs of points bordering the surface. Distances are also given in grid units and cm.

to-bottom axis). Indeed, a significant trend surface was found, involving Y and Y^2, that accounted for 10% of the variation. It forecasted high barnacle concentration in the bottom part of the plate and near the upper and lower margins. Residuals from this equation were calculated and used in spatial autocorrelation analysis.

Euclidean distances were computed among pixels; following Sturge's rule (eq. 13.3), the distances were divided into 14 classes (Fig. 13.6b). Significant positive autocorrelation was found in the first distance classes of the correlograms (Fig. 13.6c, d), supporting the hypothesis of patchiness. The size of the patches, or "range of influence" (i.e. the distance between zones of high and low concentrations), is indicated by the distance at which the first maximum negative autocorrelation value is found. This occurs in classes 4 and 5, which corresponds to a distance of about 5 in grid units, or 8 to 10 cm. The patches of high concentration are shaded on the map of the plate of artificial substrate (Fig. 13.6a).

In anisotropic situations, directional correlograms should be computed in two or several directions. Description of how the pairs of points are chosen is deferred to Subsection 3 on variograms. One may choose to represent either a single, or several of

these correlograms, one for each of the aiming geographic directions, as seems fit for the problem at hand. A procedure for representing in a single figure the directional correlograms computed for several directions of a plane has been proposed by Oden & Sokal (1986); Legendre & Fortin (1989) give an example for vegetation data. Another method is illustrated in Rossi *et al.* (1992).

Another way to approach anisotropic problems is to compute two-dimensional spectral analysis. This method, described by Priestley (1964), Rayner (1971), Ford (1976), Ripley (1981) and Renshaw & Ford (1984), differs from spatial autocorrelation analysis in the structure function it uses. As in time-series spectral analysis (Section 12.5), the method assumes the data to be stationary (second-order stationarity; i.e. no "true gradient" in the data) and made of a combination of sine patterns. An autocorrelation function $r_{dX,dY}$ for all combinations of lags (dX, dY) in the two geographic axes of a plane, as well as a periodogram with intensity I for all combinations of frequencies in the two directions of the plane, are computed. Details of the calculations are also given in Legendre & Fortin (1989), with an example.

3 — Variogram

Like correlograms, semi-variograms (called *variograms* for simplicity) decompose the spatial (or temporal) variability of observed variables among distance classes. The structure function plotted as the ordinate, called *semi-variance*, is the numerator of eq. 13.2:

$$\gamma(d) = \frac{1}{2W} \sum_{h=1}^{n} \sum_{i=1}^{n} w_{hi} (y_h - y_i)^2 \quad \text{for } h \neq i \qquad \textbf{(13.9)}$$

or, for symmetric distance and weight matrices,

$$\gamma(d) = \frac{1}{2W} \sum_{h=1}^{n-1} \sum_{i=h+1}^{n} w_{hi} (y_h - y_i)^2 \qquad \textbf{(13.10)}$$

$\gamma(d)$ is thus a non-standardized form of Geary's c coefficient. γ may be seen as a measure of the error mean square of the estimate of y_i using a value y_h distant from it by d. The two forms lead to the same numerical value in the case of symmetric distance and weight matrices. The calculation is repeated for different values of d. This provides the *sample variogram*, which is a plot of the empirical values of variance $\gamma(d)$ as a function of distance d.

The equations usually found in the geostatistical literature look a bit different, but they correspond to the same calculations:

$$\gamma(d) = \frac{1}{2W(d)} \sum_{i=1}^{W(d)} (y_i - y_{i+d})^2 \qquad \text{or} \qquad \gamma(d) = \frac{1}{2W(d)} \sum_{(h,\,i)\,|\,d_{hi} \approx d}^{W(d)} (y_h - y_i)^2$$

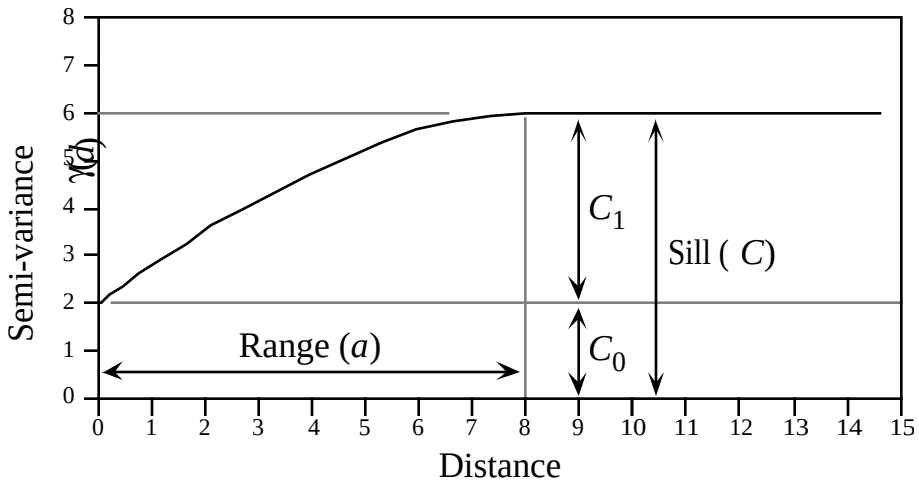

Figure 13.7 Spherical variogram model showing characteristic features: nugget effect ($C_0 = 2$ in this example), spatially structured component ($C_1 = 4$), sill ($C = C_0 + C_1 = 6$), and range ($a = 8$).

Both of these expressions mean that pairs of values are selected to be at distance d of each other; there are $W(d)$ such pairs for any given distance class d. The condition $d_{hi} \approx d$ means that distances may be grouped into distance classes, placing in class d the individual distances d_{hi} that are approximately equal to d. In directional variograms (below), d is a directional measure of distance, i.e. taken in a specified direction only. The semi-variance function is often called the variogram in the geostatistical literature. When computing a variogram, one assumes that the autocorrelation function applies to the entire surface under study (intrinsic hypothesis, Subsection 13.1.1).

Generally, variograms tend to level off at a *sill* which is equal to the variance of the variable (Fig. 13.7); the presence of a sill implies that the data are second-order stationary. The distance at which the variance levels off is referred to as the *range* (parameter a); beyond that distance, the sampling units are not spatially correlated. The discontinuity at the origin (non–zero intercept) is called the *nugget effect*; the geostatistical origin of the method transpires in that name. It corresponds to the local variation occurring at scales finer than the sampling interval, such as sampling error, fine-scale spatial variability, and measurement error. The nugget effect is represented by the error term ε_{ij} in spatial structure model 1b of Subsection 1.1.1. It describes a portion of variation which is not autocorrelated, or is autocorrelated at a scale finer than can be detected by the sampling design. The parameter for the nugget effect is C_0 and the spatially structured component is represented by C_1; the sill, C, is equal to $C_0 + C_1$. The *relative nugget effect* is $C_0/(C_0 + C_1)$.

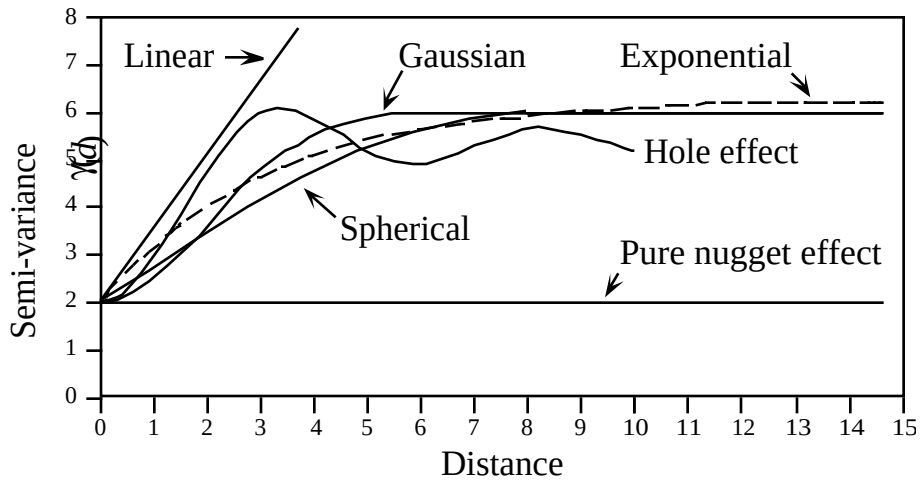

Figure 13.8 Commonly used variogram models.

Although a sample variogram is a good descriptive summary of the spatial contiguity of a variable, it does not provide all the semi-variance values needed for kriging (Subsection 13.2.2). A model must be fitted to the sample variogram; the model will provide values of semi-variance for all the intermediate distances. The most commonly used models are the following (Fig. 13.8):

- Spherical model: $\gamma(d) = C_0 + C_1\left[1.5\frac{d}{a} - 0.5\left(\frac{d}{a}\right)^3\right]$ if $d \le a$; $\gamma(d) = C$ if $d > a$.

- Exponential model: $\gamma(d) = C_0 + C_1\left[1 - \exp\left(-3\,\frac{d}{a}\right)\right]$.

- Gaussian model: $\gamma(d) = C_0 + C_1\left[1 - \exp\left(-3\,\frac{d^2}{a^2}\right)\right]$.

- Hole effect model: $\gamma(d) = C_0 + C_1\left[1 - \frac{\sin(ad)}{ad}\right]$. An equivalent form is $\gamma(d) = C_0 + C_1\left[1 - \frac{a'\sin(d/a')}{d}\right]$ where $a' = 1/a$. $(C_0 + C_1)$ represents the value of γ towards which the dampening sine function tends to stabilize. This equation would adequately model a variogram of the periodic structures in Fig. 13.5a-b (variograms only differ from Geary's correlograms by the scale of the ordinate).

• Linear model: $\gamma(d) = C_0 + bd$ where b is the slope of the variogram model. A linear model with sill is obtained by adding the specification: $\gamma(d) = C$ if $d \geq a$.

• Pure nugget effect model: $\gamma(d) = C_0$ if $d > 0$; $\gamma(d) = 0$ if $d = 0$. The second part applies to a point estimate. In practice, observations have the size of the sampling grain (Section 13.0); the error at that scale is always larger than 0.

Other less-frequently encountered models are described in geostatistics textbooks. A model is usually chosen on the basis of the known or assumed process having generated the spatial structure. Several models may be added up to fit any particular sample variogram. Parameters are fitted by weighted least squares; the weights are function of the distance and the number of pairs in each distance class (Cressie, 1991).

Anisotropy

As mentioned at the beginning of Subsection 2, anisotropy is present in data when the autocorrelation function is not the same for all geographic directions considered (David, 1977; Isaaks & Srivastava, 1989). In *geometric anisotropy*, the variation to be expected between two sites distant by d in one direction is equivalent to the variation expected between two sites distant by $b \times d$ in another direction. The range of the variogram changes with direction while the sill remains constant. In a river for instance, the kind of variation expected in phytoplankton concentration between two sites 5 m apart across the current may be the same as the variation expected between two sites 50 m apart along the current even though the variation can be modelled by spherical variograms with the same sill in the two directions. Constant b is called the *anisotropy ratio* ($b = 50/5 = 10$ in the river example). This is equivalent to a change in distance units along one of the axes. The anisotropy ratio may be represented by an ellipse or a more complex figure on a map, its axes being proportional to the variation expected in each direction. In *zonal anisotropy*, the sill of the variogram changes with direction while the range remains constant. An extreme case is offered by a strip of land. If the long axis of the strip is oriented in the direction of a major environmental gradient, the variogram may correspond to a linear model (always increasing) or to a spherical model with a sill larger than the nugget effect, whereas the variogram in the direction perpendicular to it may show only random variation without spatial structure with a sill equal to the nugget effect.

Directional variogram and correlogram

Directional variograms and correlograms may be used to determine whether anisotropy (defined in Subsection 2) is present in the data; they may also be used to describe anisotropic surfaces or to account for anisotropy in kriging (Subsection 13.2.2). A direction of space is chosen (i.e. an angle θ, usually by reference to the geographic north) and a search is launched for the pairs of points that are within a given distance class d in that direction. There may be few such pairs perfectly aligned in the aiming direction, or none at all, especially when the observed sites are not regularly spaced on the map. More pairs can usually be found by looking within a small neighbourhood around the aiming line (Fig. 13.9). The neighbourhood is determined by an angular tolerance parameter φ and a parameter κ that sets the tolerance for distance classes along the aiming line. For each observed point $Ø_h$ in turn, one looks for other points $Ø_i$ that are at distance $d \pm \kappa$ from it. All points found

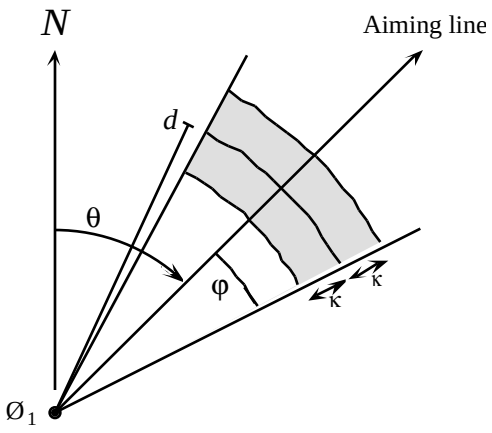

Figure 13.9 Search parameters for pairs of points in directional variograms and correlograms. From an observed study site $Ø_1$, an aiming line is drawn in the direction determined by angle θ (usually by reference to the geographic north, indicated by N). The angular tolerance parameter φ determines the search zone (grey) laterally whereas parameter κ sets the tolerance along the aiming line for each distance class d. Points within the search window (in gray) are included in the calculation of $I(d)$, $c(d)$ or $\gamma(d)$.

within the search window are paired with the reference point $Ø_h$ and included in the calculation of semi-variance or spatial autocorrelation coefficients for distance class d. In most applications, the search is bi-directional, meaning that one also looks for points within a search window located in the direction opposite (180°) the aiming direction. Isaaks & Srivastava (1989, Chapter 7) propose a way to assemble directional measures of semi-variance into a single table and to produce a contour map that describes the anisotropy in the data, if any; Rossi *et al.* (1992) have used the same approach for directional spatial correlograms.

Numerical example. An artificial data set was produced containing random autocorrelated data. The data were generated using the turning bands method (David, 1977; Journel & Huijbregts, 1978); random normal deviates were autocorrelated following a spherical model with a range of 5. Pure spatial autocorrelation, as described in the spatial structure model 1b of Subsection 1.1.1, generates continuity in the data (Fig. 13.10a). The variogram (without test of significance) and spatial correlograms (with tests) are presented in Figs. 13.10b-d. In this example, the data were standardized during data generation, prior to spatial autocorrelation analysis, so that the denominator of eq. 13.2 is 1; therefore, the variogram and Geary's correlogram are identical. The variogram suggests a spherical model with a range of 6 units and a small nugget effect (Fig. 13.10b).

Besides the description of spatial structures, variograms are used for several other purposes in spatial analysis. In Subsection 13.2.2, they will be the basis for interpolation by kriging. In addition, structure functions (variograms, spatial

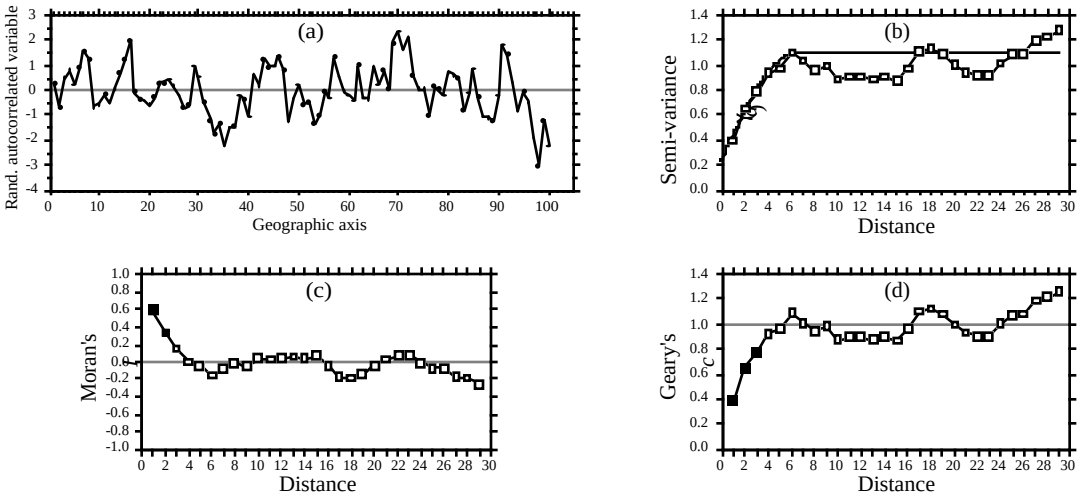

Figure 13.10 (a) Series of 100 equispaced random, spatially autocorrelated data. (b) Variogram, with spherical model superimposed (heavy line). Abscissa: distances between points along the geographic axis in (a). (c) and (d) Spatial correlograms. Dark squares: autocorrelation statistics that remain significant after progressive Bonferroni correction ($\alpha = 0.05$); white squares: non-significant values.

correlograms) may prove extremely useful to help determine the grain size of the sampling units and the sampling interval to be used in a survey, based upon the analysis of a pilot study. They may also be used to perform change-of-scale operations and predict the type of autocorrelation and variance that would be observed if the grain size of the sampling design was different from that actually used in a field study (Bellehumeur *et al.*, 1997).

4 — Spatial covariance, semi-variance, correlation, cross-correlation

This Subsection examines the relationships between spatial covariance, semi-variance and correlation (including cross-correlation), under the assumption of second-order stationarity, leading to the concept of cross-correlation. This assumption (Subsection 13.2.1) may be restated as follows:

- The first moment (mean of points *i*) of the variable exists:

$$\mathrm{E}\,[y_i] \;=\; \frac{1}{n}\sum_{i\,=\,1}^{n} y_i \;=\; m_i \qquad \textbf{(13.11)}$$

Its value does not depend on position in the study area.

- The second moment (covariance, numerator of eq. 13.1) of the variable exists:

$$C(d) = \left[\frac{1}{W(d)} \sum_{(h,i)\,|\,d_{hi} \approx d}^{W(d)} y_h y_i \right] - m_h m_i \qquad \textbf{(13.12)}$$

$$C(d) = \mathrm{E}[y_h y_i] - m^2 \quad \text{for } h, i \,|\, d_{hi} \approx d \qquad \textbf{(13.13)}$$

The value of $C(d)$ depends only on d and on the orientation of the distance vector, but not on position in the study area. To understand eq. 13.12 as a measure of covariance, imagine the elements of the various pairs y_h and y_i written in two columns as if they were two variables. The equation for the covariance (eq. 4.4) may be written as follows, using a final division by n instead of $(n-1)$ (maximum-likelihood estimate of the covariance, which is standard in geostatistics):

$$s_{y_h y_i} = \frac{\sum y_h y_i}{n} - \frac{\sum y_h \sum y_i}{n\ n} = \frac{\sum y_h y_i}{n} - m_h m_i$$

The overall variance (Var, with division by n instead of $n-1$) also exists since it is the covariance calculated for $d = 0$:

$$\mathrm{Var}[y_i] = \mathrm{E}[y_i - m_i]^2 = C(0) \qquad \textbf{(13.14)}$$

When computing the semi-variance, one only considers pairs of observations distant by d. Eqs. 13.9 and 13.10 are re-written as follows:

$$\gamma(d) = \frac{1}{2}\mathrm{E}[y_h - y_i]^2 \quad \text{for } h, i \,|\, d_{hi} \approx d \qquad \textbf{(13.15)}$$

A few lines of algebra obtain the following formula:

$$\gamma(d) = \frac{\sum y_i^2 - \sum y_h y_i}{W(d)} = C(0) - C(d) \quad \text{for } h, i \,|\, d_{hi} \approx d \qquad \textbf{(13.16)}$$

Two properties are used in the derivation: (1) $\sum y_h = \sum y_i$, and (2) the variance (Var, eq. 13.14) can be estimated using any subset of the observed values if the hypothesis of second-order stationarity is verified.

The correlation is the covariance divided by the product of the standard deviations (eq. 4.7). For a spatial process, the (auto)correlation is written as follows (leading to eq. 13.1):

$$r(d) = \frac{C(d)}{s_h s_i} = \frac{C(d)}{\mathrm{Var}[y_i]} = \frac{C(d)}{C(0)} \qquad \textbf{(13.17)}$$

Consider the formula for Geary's c (eq. 13.2), which is the semi-variance divided by the overall variance. The following derivation:

$$c(d) = \frac{\gamma(d)}{\mathrm{Var}[y_i]} = \frac{C(0) - C(d)}{C(0)} = 1 - \frac{C(d)}{C(0)} = 1 - r(d)$$

leads to the conclusion that Geary's c is one minus the coefficient of spatial (auto)correlation. In a graph, the semi-variance and Geary's c coefficient have exactly the same shape (e.g. Figs. 13.10b and d); only the ordinate scales may differ. An autocorrelogram plotted using $r(d)$ has the exact reverse shape as a Geary correlogram. An important conclusion is that the plots of semi-variance, covariance, Geary's c coefficient, and $r(d)$, are equivalent to characterize spatial structures under the hypothesis of second-order stationarity (Bellehumeur & Legendre, 1998).

Cross-covariances may also be computed from eq. 13.12, using values of *two different variables* observed at locations distant by d (Isaaks & Srivastava, 1989). Eq. 13.17 leads to a formula for cross-correlation which may be used to plot cross-correlograms; the construction of the correlation statistic is the same as for time series (eq. 12.10). With transect data, the result is similar to that of eq. 12.10. However, the programs designed to compute spatial cross-correlograms do not require the data to be equispaced, contrary to programs for time-series analysis. The theory is presented by Rossi *et al.* (1992), as well as applications to ecology.

Ecological application 13.1b

A survey was conducted on a homogeneous sandflat in the Manukau Harbour, New Zealand, to identify the scales at which spatial heterogeneity could be detected in the distribution of adult and juvenile bivalves (*Macomona liliana* and *Austrovenus stutchburyi*), as well as indications of adult-juvenile interactions within and between species. The results were reported by Hewitt *et al.* (1997); see also Ecological application 13.2. Sampling was conducted along transects established at three sites located within a 1-km^2 area; there were two transects at each site, forming a cross. Sediment cores (10 cm diam., 13 cm deep) were collected using a nested sampling design; the basic design was a series of cores 5 m apart, but additional cores were taken 1 m from each of the 5-m-distant cores. This design provided several comparison in the short distance classes (1, 4, 5, and 6 m). Using transects instead of rectangular areas allowed relatively large distances (150 m) to be studied, given the allowable sampling effort. Nested sampling designs have also been advocated by Fortin *et al.* (1989) and by Bellehumeur & Legendre (1998).

Spatial correlograms were used to identify scales of variation in bivalve concentrations. The Moran correlogram for juvenile *Austrovenus*, computed for the three transects perpendicular to the direction of tidal flow, displayed significant spatial autocorrelation at distances of 1 and 5 m (Fig. 13.11a). The same pattern was found in the transects parallel to tidal flow. Figure 13.11a also indicates that the range of influence of autocorrelation was about 15 m. This was confirmed by plotting bivalve concentrations along the transects: LOWESS smoothing of the graphs (Subsection 10.3.8) showed patches of about 25-30 m in diameter (Hewitt *et al.*, 1997, Figs. 3 and 4).

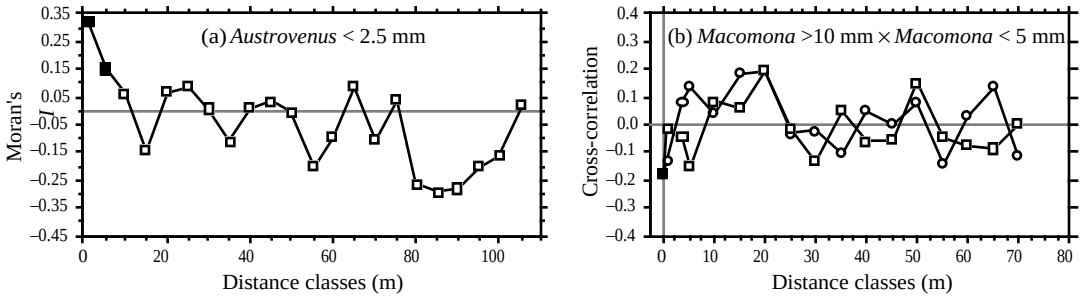

Figure 13.11 (a) Spatial autocorrelogram for juvenile *Austrovenus* densities. (b) Cross-correlogram for adult-juvenile *Macomona* interactions, folded about the ordinate: circles = positive lags, squares = negative lags. Dark symbols: correlation statistics that are significant after progressive Bonferroni correction ($\alpha = 0.05$). Redrawn from Hewitt *et al*. (1997).

Cross-correlograms were computed to detect signs of adult-juvenile interactions. In the comparison of adult (> 10 mm) to juvenile *Macomona* (< 5 mm), a significant negative cross-correlation was identified at 0 m in the direction parallel to tidal flow (Fig. 13.11b); correlation was not significant for the other distance classes. As in time series analysis, the cross-correlation function is not symmetrical; the correlation obtained by comparing values of $\mathbf{y}_1$ to values of $\mathbf{y}_2$ located at distance d on their right is not the same as when values of $\mathbf{y}_2$ are compared to values of $\mathbf{y}_1$ located at distance d on their right, except for $d = 0$. In Fig. 13.11b, the cross-correlogram is folded about the ordinate (compare to Fig. 12.9). Contrary to time series analysis, it is not useful in spatial analysis to discuss the direction of lag of a variable with respect to the other unless one has a specific hypothesis to test.

5 — Multivariate Mantel correlogram

Sokal (1986) and Oden & Sokal (1986) found an ingenious way to compute a correlogram for multivariate data, using the normalized Mantel statistic r_M and test of significance (Subsection 10.5.1). This method is useful, in particular, to describe the spatial structure of species assemblages.

The principle is to quantify the ecological relationships among sampling sites by means of a matrix $\mathbf{Y}$ of multivariate similarities or distances (using, for instance, coefficients S_{17} or D_{14} in the case of species abundance data), and compare $\mathbf{Y}$ to a *model matrix* $\mathbf{X}$ (Subsection 10.5.1) which is different for each geographic distance class (Fig. 13.12).

- For distance class 1 for instance, pairs of neighbouring stations (that belong to the first class of geographic distances) are coded 1, whereas the remainder of matrix $\mathbf{X}_1$ contains zeros. A first Mantel statistic (r_{M1}) is calculated between $\mathbf{Y}$ and $\mathbf{X}_1$.

- The process is repeated for the other distance classes d, building each time a model-matrix $\mathbf{X}_d$ and recomputing the normalized Mantel statistic. Matrix $\mathbf{X}_d$ may contain 1's

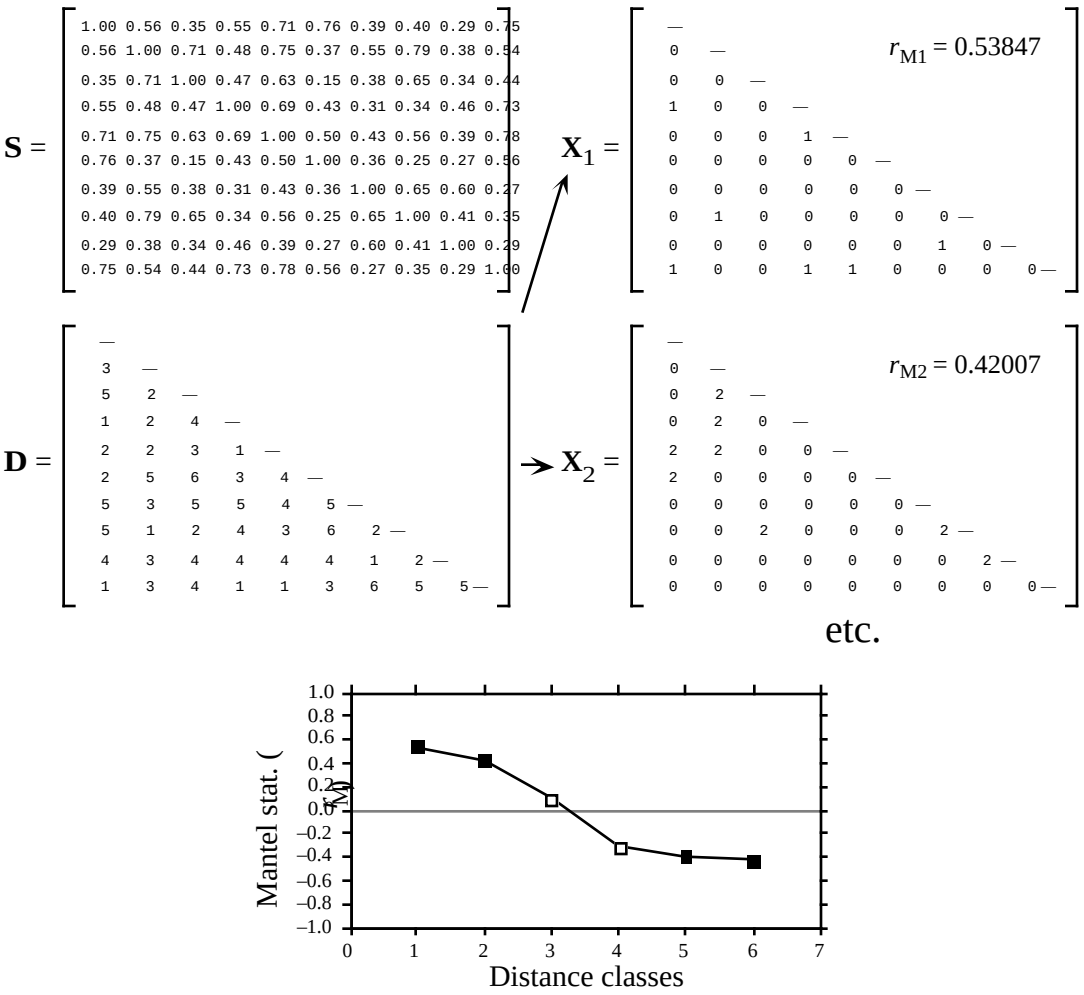

Figure 13.12 Construction of a Mantel correlogram for a similarity matrix **S** ($n = 10$ sites). The matrix of geographic distance classes **D**, from Fig. 13.4, gives rise to model matrices $\mathbf{X}_1$, $\mathbf{X}_2$, etc. for the various distance classes d. These are compared, in turn, to matrix $\mathbf{Y} = \mathbf{S}$ using standardized Mantel statistics (r_{Md}). Dark symbols in the correlogram: Mantel statistics that are significant after progressive Bonferroni correction ($\alpha = 0.05$).

for pairs that are in the given distance class, or the code value for that distance class (d), or any other value different from zero; all coding methods lead to the same value of the normalized Mantel statistic r_M.

The Mantel statistics, plotted against distance classes, produce a multivariate correlogram. Each value is tested for significance in the usual way, using either

permutations or Mantel's normal approximation (Box 10.2). Computation of standardized Mantel statistics assumes second-order stationarity. As in the case of univariate correlograms (above), one is advised to use some form of correction for multiple testing before interpreting Mantel correlograms.

Numerical example. Consider again the 10 sampling sites of Fig. 13.4. Assume that species assemblage data were available and produced similarity matrix **S** of Fig. 13.12. Matrix **S** played here the role of **Y** in the computation of Mantel statistics. Were the species data autocorrelated? Distance matrix **D**, already divided into 6 classes in Fig. 13.4, was recoded into a series of model matrices $\mathbf{X}_d$ (d = 1, 2, etc.). In each of these, the pairs of sites that were in the given distance class received the value d, whereas all other pairs received the value 0. Mantel statistics were computed between **S** and each of the $\mathbf{X}_d$ matrices in turn; positive and significant Mantel statistics indicate positive autocorrelation in the present case. The statistics were tested for significance using 999 permutations and plotted against distance classes d to form the Mantel correlogram. The progressive Bonferroni method was used to account for multiple testing because interest was primarily in detecting autocorrelation in the first distance classes.

Before computing the Mantel correlogram, one must assume that the condition of second-order stationarity is satisfied. This condition is more difficult to explain in the case of multivariate data; it means essentially that the surface is uniform in (multivariate) mean and variance at broad scale. The correlogram illustrated in Fig. 13.12 suggests the presence of a gradient. If the condition of second-order-stationarity is satisfied, this means that the gradient detected by this analysis is a part of a larger, autocorrelated spatial structure. This was called a "false gradient" in the numerical example of Subsection 2, above.

When **Y** is a similarity matrix and distance classes are coded as described above, positive Mantel statistics correspond to positive autocorrelation; this is the case in the numerical example. When the values in **Y** are distances instead of similarities, or if the 1's and 0's are interchanged in matrix **X**, the signs of all Mantel statistics are changed. One should always specify whether positive autocorrelation is expressed by positive or negative values of the Mantel statistics when presenting Mantel correlograms. The method was applied to vegetation data by Legendre & Fortin (1989).